Mellin-Transform-Based Performance Analysis of FFH M-ary FSK Using Product Combining for Combatting Partial-Band Noise Jamming

Sohail Ahmed, Lie-Liang Yang, *Senior Member, IEEE*, and Lajos Hanzo, *Fellow, IEEE*

***Abstract*—We employ the Mellin transform to facilitate the bit error ratio (BER) analysis of a fast frequency hopping (FFH)-assisted, M-ary frequency-shift keying (MFSK) using product combining (PC) when the transmitted signal is subjected to both Rayleigh fading and partial-band noise jamming. Exploiting the fact that the Mellin transform of the product of independent random variables is the product of their Mellin transforms, we derive the probability density function (PDF) of the PC's output. The derivation of the PDF then allows the computation of the system's BER. It is shown that the Mellin transform substantially simplifies the analysis of the PC receiver and hence facilitates, for the first time, the analysis of the FFH-MFSK PC receiver for modulation orders of $M > 2$.**

***Index Terms*—Fast frequency hopping (FFH), Mellin transform, partial-band noise jamming (PBNJ), probability density function (PDF), product combining (PC), Rayleigh fading, residues.**

I. Introduction

FAST FREQUENCY hopping (FFH), M-ary frequency-shift keying (MFSK) using product combining (PC) has been shown to efficiently combat partial-band noise jamming (PBNJ) [1]–[8]. In [3] and [5]–[7], Teh *et al.*, Chang and Tu, Shen and Su, and Lim *et al.* have analyzed the PC-based FFH binary frequency-shift keying (BFSK) receiver under various fading and jamming conditions, employing the characteristic function (CF) [9] and using the natural logarithm to convert the product into summation for the sake of deriving the probability density function (PDF) of the PC's output. The challenge associated with the natural logarithm and CF-based approach is that, closed-form expressions cannot be readily obtained for the PDF of the PC's output. Consequently, the symbol error probability (SEP) of BFSK is expressed using a double integral [3]. For the more challenging MFSK scenario, the corresponding expression is expected to be more complicated, involving multiple integrals.

Let us elaborate on this point using the relevant expressions for the PDF of the PC's output and for the SEP. In the context of the CF and the natural-logarithm-based method employed in [1]–[5], if

$$Z_m = \prod_{l=0}^{L-1} U_{ml} \tag{1}$$

denotes the PC's output, we have

$$\ln Z_m = \sum_{l=0}^{L-1} \ln U_{ml} \tag{2}$$

where U_{ml} denotes the energy detector output, L is the number of FFH hops per symbol, and $m = 0, 1, \ldots, M-1$. Hence, the PDF of $\ln Z_m$ is derived in terms of the PDFs of $\ln U_{ml}$ using the CF method [3], [7], [9]. Thus, we have

$$\phi(\ln Z_m) = \prod_{l=0}^{L-1} \phi(\ln U_{ml}) \tag{3}$$

where $\phi(x)$ denotes the CF of x. The PDF of $\ln Z_m$ can then be obtained from its CF [9]. To determine the PDF $f_{Z_m}(y_m)$ of the PC output Z_m from the PDF of $\ln Z_m$, further mathematical steps are involved. For the sake of bit error ratio (BER) calculation, the SEP is derived in the context of MFSK-based schemes using the relation [9]

$$P_s = 1 - \int_0^\infty f_{Z_0}(y_0) \left[\int_0^{y_0} f_{Z_m}(y_m) dy_m \right]^{M-1} dy_0 \tag{4}$$

given that $m = 0$ is the transmitted tone. For BFSK, i.e., for $M = 2$, the relation given by (4) is equivalent to finding the probability that $(Z_1 > Z_0)$. The natural-logarithm-based method of [3] and [7] instead finds the probability that $(\ln Z_1 > \ln Z_0)$. Alternatively, some simpler technique may be invoked, such as finding the probability that $\ln(Z_1 - Z_0) > 0$ [7], thus obviating the need to find the PDF of the PC output Z_m. However, for modulation orders greater than 2, the analysis invloves $M > 2$ decision variables, and no similar *shortcut* may be applied. Thus, if $M > 2$ is considered, (4) would consist of four integrals. This is the reason that the natural logarithm method [3], [7] has not been applied to modulation orders greater than 2.

In [8], the employment of Fox's H-functions was proposed for deriving the PDF of the PC's output and, hence, the BER of the FFH-BFSK PC receiver. In their analysis, Huo and Aluoini

Manuscript received October 24, 2006; revised August 29, 2007 and October 4, 2007. This work was supported in part by the Higher Education Commission, Pakistan, by the Engineering and Physical Sciences Research Council, U.K., and by the European Union under the auspices of the Phoenix and Newcom projects. The review of this paper was coordinated by Prof. H.-C. Wu.

S. Ahmed is with the College of Aeronautical Engineering, Risalpur 24080, Pakistan (e-mail: ahmed@mail.au.edu.pk).

L.-L. Yang and L. Hanzo are with the School of Electronics and Computer Science, University of Southampton, SO17 1BJ Southampton, U.K. (e-mail: lly@ecs.soton.ac.uk; lh@ecs.soton.ac.uk).

Digital Object Identifier 10.1109/TVT.2007.912604

[8] have exploited the fact that a product of H-functions is also an H-function [10]. Huo and Aluoini [8] have also employed another technique, which involves generalized F-variates for the sake of deriving the corresponding BER expressions. The methods proposed in [8] have been shown to be unproblematic for BFSK systems. However, they might lead to more computationally cumbersome formulas when applied to higher throughput M-ary systems.

Hence, all the analysis techniques proposed in the literature for PC-based receivers [3], [7], [8] have been applied to BFSK and are unsuitable for a modulation order of $M > 2$. Motivated by the fact that the Mellin transform may be employed to derive the PDF of a product of random variables [10]–[12], we invoke, for the first time in a journal, this powerful technique that analyzes a PC-aided FFH-MFSK. To elaborate a little further, the Mellin transform is an integral transform similar to the Laplace and Fourier transforms. Explicitly, the Mellin transform of a random variable having a PDF of $f(x)$ is given by [10], [12]

$$\mathcal{M}\left[f(x), z\right] = \int_0^\infty x^{z-1} f(x) dx \tag{5}$$

whereas the corresponding inverse Mellin transform returns the PDF and is defined as [10], [12]

$$f(x) = \frac{1}{2\pi i} \int_{c-i\infty}^{c+i\infty} x^{-z} \mathcal{M}\left[f(x), z\right] dz \tag{6}$$

where we have $i = \sqrt{-1}$, and the integration is carried out along any line parallel to the imaginary axis that lies within the strip of analyticity [10].

The novel goal of this paper is for *the proposed Mellin-transform-based technique to allow the PDF of the PC's output to be expressed in semiclosed form and thereby to substantially simplify the BER analysis of FFH-aided MFSK using PC when the transmitted signal is corrupted by PBNJ and Rayleigh fading and, hence to facilitate, for the first time, its analysis for* $M > 2$. In our previous contribution on this topic [13], we considered the same problem, employing the square-law detection [9] of the FFH-MFSK signal. By contrast, in this contribution, we employ envelope detection [9] because the choice of either the square-law detector or the envelope detector does not affect the system's BER, and both of them may be considered for employment in a noncoherent MFSK demodulator [9]. However, as demonstrated in Section IV, employing an envelope detector in the MFSK demodulator results in a more convenient computation of the BER for a wide range of system parameters.

Furthermore, we will show in Section III that for envelope detection, the random variable at the PC's output is a product of Rayleigh variables, whereas in [13], it was characterized by a product of exponentially distributed variables. In [14], the PDF of a product of Rayleigh-distributed variables has been derived by employing the Mellin transform. However, the inverse of the Mellin transform has been derived using Meijer's G-function in [14], whereas we will employ the residue method for this purpose, owing to its conceptual simplicity [11], [13].

The rest of this paper is structured as follows. In Section II, the system under study is briefly described. In Section III, the relevant statistics, as well as the corresponding BER expressions, are derived using the Mellin transform. In Section IV, our numerical results are discussed, and finally, in Section V, our conclusions are presented.

II. System Description

The system studied is similar to that considered in [3] and [8], except that we have a modulation order of $M \geq 2$. In the FFH-MFSK transmitter, the MFSK signal modulates the carrier generated by a frequency synthesizer, which is controlled by the L-tuple FFH address generated by a pseudonoise (PN) generator, where L is the number of frequency hops per symbol. The hop interval T_h is related to the symbol interval T_s by $T_h = T_s/L$. The separation between adjacent frequency tones is assumed to be $R_h = 1/T_h$, which also represents the bandwidth occupied by a single FFH-MFSK tone.

The channel is assumed to be a frequency-flat Rayleigh-fading medium for each of the transmitted frequencies. Furthermore, we assume that the separation between the adjacent frequencies is higher than the coherence bandwidth of the channel. Therefore, all FFH tones conveying the same symbol experience independent fading.

The transmitted signal is also corrupted by additive white Gaussian noise (AWGN) and a PBNJ signal having single-sided power spectral densities of N_0 and N_J, respectively. We assume that the PBNJ signal jams a fraction $0 \leq \rho \leq 1$ [8] of the total spread-spectrum bandwidth W_{ss}. We also assume that the PBNJ signal is contiguous, and hence, all of the MFSK tones of a particular band are jammed if the jamming signal is present in that band. Thus, the probability that a band or a tone is jammed is given by ρ, whereas the probability that the band is not jammed is $(1 - \rho)$.

The receiver schematic is shown in Fig. 1, where a bandpass filter removes any frequency that falls outside the bandwidth W_{ss}. Then, the frequency dehopper of Fig. 1, which is identical to and aligned with the frequency hopper of the transmitter, despreads the received signal by exploiting the knowledge of the transmitter's unique FFH address. The demodulator is comprised of M branches, each corresponding to a single MFSK tone and consisting of an envelope detector [9], as well as a PC. At the output of the PC, one of the M decision variables is obtained.

III. BER Analysis

In this section, we outline the PDFs of the envelope detector outputs and employ the Mellin transform for deriving the PDFs and cumulative distribution functions (CDFs) of the PC's outputs. Finally, these PDFs and CDFs will assist us in computing the BER [9].

When the FFH-MFSK signal suffers from Rayleigh fading, the output of the noncoherent envelope detector is also Rayleigh distributed [9]. Therefore, assuming that the first of the M tones

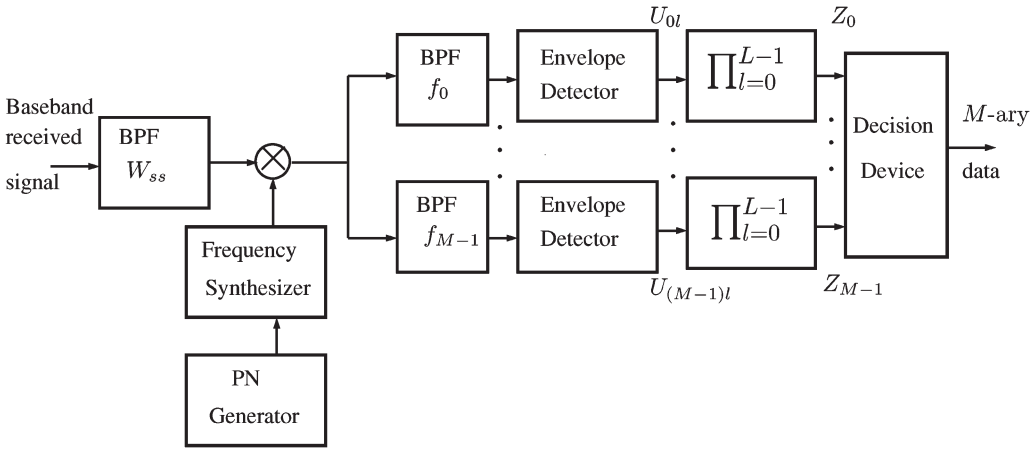

Fig. 1. FFH-MFSK receiver using PC.

is activated by the transmitter, it can be shown that the PDF of the envelope detector's output signal U_{ml}, $m = 0, 1, \ldots, M-1, l = 0, 1, \ldots, L-1$, corresponding to the desired signal tone, when the transmitted signal is jammed by PBNJ, is given by [8], [9]

$$f_{U_{0l}}^{(J)}(x) = \frac{x}{2\left(\sigma_0^2 + \sigma_J^2\right)\left(1+\gamma_{ht}\right)} \times \exp\left(\frac{-x^2}{2\left[\sigma_0^2+\sigma_J^2\right]\left[1+\gamma_{ht}\right]}\right), \qquad x \geq 0 \quad (7)$$

where $\gamma_{ht} = bE_b/(N_T L)$ is the signal-to-interference-plus-noise ratio per hop, $N_T = N_0 + N_J/\rho$, E_b is the transmitted energy per bit, and $b = \log_2 M$ is the number of bits per symbol. Furthermore, in (7), the superscript (J) explicitly indicates that the tone suffers from PBNJ, and $\sigma_0^2 = R_h N_0$ and $\sigma_J^2 = R_h N_J/\rho$ represent the variance of the AWGN and the PBNJ, respectively.

By contrast, when the signal is not jammed, the corresponding PDF can be expressed as [8], [9]

$$f_{U_{0l}}(x) = \frac{x}{2\sigma_0^2(1+\gamma_h)} \exp\left(\frac{-x^2}{2\sigma_0^2[1+\gamma_h]}\right), \qquad x \geq 0 \quad (8)$$

where $\gamma_h = bE_b/(N_0 L)$ is the signal-to-noise ratio (SNR) per hop. Similarly, the corresponding expressions for the PDFs of the undesired tones of $m = 1, 2, \ldots, M-1$ are given by [8], [9]

$$f_{U_{ml}}^{(J)}(x) = \frac{x}{2\left(\sigma_0^2+\sigma_J^2\right)} \exp\left(\frac{-x^2}{2\left[\sigma_0^2+\sigma_J^2\right]}\right), \quad x \geq 0, m > 0 \quad (9)$$

and

$$f_{U_{ml}}(x) = \frac{x}{2\sigma_0^2} \exp\left(\frac{-x}{2\sigma_0^2}\right), \quad x \geq 0, m > 0. \quad (10)$$

Therefore, the Mellin transforms of the PDFs given by (7)–(10) may be expressed using (5) as [10], [13], [15]

$$\mathcal{M}\left[f_{U_{0l}^{(J)}}(x), z\right] = \alpha_J^{(1-z)/2}\Gamma(z/2+1/2) \quad (11)$$

$$\mathcal{M}\left[f_{U_{0l}}(x), z\right] = \alpha^{(1-z)/2}\Gamma(z/2+1/2) \quad (12)$$

$$\mathcal{M}\left[f_{U_{ml}^{(J)}}(x), z\right] = \beta_J^{(1-z)/2}\Gamma(z/2+1/2), \quad m > 0 \quad (13)$$

and

$$\mathcal{M}\left[f_{U_{ml}}(x), z\right] = \beta^{(1-z)/2}\Gamma(z/2+1/2), \quad m > 0 \quad (14)$$

where we have $\alpha_J = 1/[2(\sigma_0^2+\sigma_J^2)(1+\gamma_{ht})]$, $\alpha = 1/[2\sigma_0^2(1+\gamma_h)]$, $\beta_J = 1/[2(\sigma_0^2+\sigma_J^2)]$, and $\beta = 1/2\sigma_0^2$, and $\Gamma(.)$ denotes the Gamma function [16].

Assuming that p out of the L hops of a symbol are jammed, the output of the mth PC, $m = 0, 1, \ldots, M-1$, as shown in Fig. 1, may be expressed as

$$Z_m = \prod_{l=0}^{p-1} U_{ml}^{(J)} \prod_{l=0}^{L-p-1} U_{ml}. \quad (15)$$

We will now exploit the fact that *the Mellin transform of the product of independent random variables is equal to the product of the Mellin transforms of the individual random variables* [10], [17] for the sake of reducing the numerical computational complexity involved. Because the signals in all of the hops are independent, the Mellin transform of the mth PC's output, given that p out of the L hops are jammed, may be expressed as

$$\mathcal{M}\left[f_{Z_m}(y_m|p), z\right] = \left[\mathcal{M}\left[f_{U_{ml}^{(J)}}(x), z\right]\right]^p \left[\mathcal{M}\left[f_{U_{ml}}(x), z\right]\right]^{L-p} \quad (16)$$

where $f_{Z_m}(y_m|p)$ represents the PDF of the mth PC's output $m = 0, 1, \ldots, M-1$, given that p out of the L hops are jammed. Consequently, from (11), (12), and (16), for the desired signal tone, we have

$$\mathcal{M}\left[f_{Z_0}(y_0|p), z\right] = \alpha_J^{p(1-z)/2}\alpha^{(L-p)(1-z)/2}\Gamma^L(z/2+1/2) \quad (17)$$

whereas from (13) and (14), for the undesired (nonsignal) tones corresponding to $m > 0$, we have

$$\mathcal{M}\left[f_{Z_m}(y_m|p), z\right] = \beta_J^{p(1-z)/2}\beta^{(L-p)(1-z)/2}\Gamma^L(z/2+1/2). \tag{18}$$

Then, using (6), the PDF of Z_0 can be generated as the inverse Mellin transform of (17), yielding

$$f_{Z_0}(y_0|p) = \frac{1}{2\pi i}\int_{c-i\infty}^{c+i\infty} y_0^{-z}\alpha_J^{p(1-z)/2}\alpha^{(L-p)(1-z)/2} \times \Gamma^L\left[(z+1)/2\right]dz. \tag{19}$$

We now invoke the change of variable technique and replace $(z+1)/2$ by z in the above equation because this does not affect the path of integration [10]. Hence, after further simplification, we have

$$f_{Z_0}(y_0|p) = \frac{1}{\pi i}\int_{c-i\infty}^{c+i\infty} y_0^{1-2z}\alpha_J^{p(1-z)}\alpha^{(L-p)(1-z)}\Gamma^L(z)dz. \tag{20}$$

Upon applying the residue theorem in [10]–[13] and [18] to (20), we have

$$f_{Z_0}(y_0|p) = \sum_j \mathrm{Res}\left[2y_0^{1-2z}\alpha_J^{p(1-z)} \times \alpha^{(L-p)(1-z)}\Gamma^L(z)\right]_{(z=-j)} \tag{21}$$

where $\mathrm{Res}[.]_{(z=-j)}$ represents the residue at the jth pole of the integrand. The PDF of Z_0 can be determined upon numerically evaluating (21) by using symbolic-mathematics-based software such as Maple or Mathematica. However, in what follows, we also derive expressions for the PDFs $f_{Z_0}(y_0|p)$ and $f_{Z_m}(y_m|p)$, with the aid of [10], [11], [13], [16], and [18].

It is widely recognized that the function $\Gamma(z)$ has an infinite number of poles at $z = -j$ for $j = 1, 2, \ldots$, and at each of these poles, the corresponding residue is given by [16], [18]

$$\Gamma(z)(z+j)|_{(z=-j)} = \frac{(-1)^j}{j!}. \tag{22}$$

Because the $\Gamma^L(z)$ in (21) has an Lth-order pole at each integer value of $z = -j$, (21) may be expressed, using the relationship characterizing the residues of multiple poles [10], [11], [16], [18], as

$$f_{Z_0}(y_0|p) = \frac{2\alpha_J^p\alpha^{L-p}y_0}{(L-1)!}\sum_{j=0}^{\infty}\frac{d^{L-1}}{dz^{L-1}} \times \left[\left(\alpha_J^p\alpha^{L-p}y_0^2\right)^{-z}\Gamma^L(z)(z+j)^L\right]_{(z=-j)}. \tag{23}$$

Letting $\mathcal{U}(z) = (\alpha_J^p\alpha^{L-p}y_0^2)^{-z}$ and $\mathcal{V}(z) = \Gamma^L(z)(z+j)^L$ and using Leibnitz' rule [13], [16], (23) may be expressed as

$$f_{Z_0}(y_0|p) = \frac{2\alpha_J^p\alpha^{L-p}y_0}{(L-1)!}\sum_{j=0}^{\infty}\sum_{r=0}^{L-1}\binom{L-1}{r} \times \left[\mathcal{U}^{(r)}(z)\mathcal{V}^{(L-1-r)}(z)\right]_{(z=-j)} \tag{24}$$

where $\mathcal{U}^{(r)}(z)$ and $\mathcal{V}^{(r)}(z)$ denote the rth derivatives of $\mathcal{U}(z)$ and $\mathcal{V}(z)$, respectively. Then, it can be readily shown that we have

$$\mathcal{U}(z)|_{(z=-j)} = \left(\alpha_J^p\alpha^{L-p}y_0^2\right)^j \tag{25}$$

and

$$\mathcal{U}^{(r)}(z)|_{(z=-j)} = \left[-\ln\left(\alpha_J^p\alpha^{L-p}y_0^2\right)\right]^r\left(\alpha_J^p\alpha^{L-p}y_0^2\right)^j \tag{26}$$

while, following a number of manipulations with the aid of [10], [11], [13], [16], and [18], we arrive at

$$\mathcal{V}(z)|_{(z=-j)} = \frac{(-1)^{jL}}{(j!)^L} \tag{27}$$

and

$$\mathcal{V}^{(r)}(z)|_{(z=-j)} = L\left\{\sum_{t=0}^{r-1}\binom{r-1}{t}\mathcal{V}^{(t)}(z)|_{(z=-j)} \times (-1)^{r-t}(r-1-t)!\sum_{k=0}^{\infty}\left[\frac{1}{(1+k)^{r-t}}\right] + \sum_{t=0}^{r-1}\binom{r-1}{t}\mathcal{V}^{(t)}(z)|_{(z=-j)}\sum_{k=1}^{j}\frac{1}{(k)^{r-t}}\right\}. \tag{28}$$

See [13] for the complete derivation of the above equation. Hence, the PDF of Z_0, conditioned on the assumption that p out of the L hops are jammed, can be determined from (24), whereas the PDF of $Z_m m > 0$ can be similarly expressed as [10], [11], [13], [16], [18]

$$f_{Z_m}(y_m|p) = \frac{2\beta_J^p\beta^{L-p}y_m}{(L-1)!}\sum_{j=0}^{\infty}\sum_{r=0}^{L-1}\binom{L-1}{r} \times \left[\mathcal{U}_m^{(r)}(z)\mathcal{V}^{(L-1-r)}(z)\right]_{(z=-j)} \tag{29}$$

where

$$\mathcal{U}_m(z)|_{(z=-j)} = \left(\beta_J^p\beta^{L-p}y_m^2\right)^j \tag{30}$$

$$\mathcal{U}_m^{(r)}(z)|_{(z=-j)} = [-\ln(\beta_J^p\beta^{L-p}y_m^2)]^r(\beta_J^p\beta^{L-p}y_m^2)^j. \tag{31}$$

Given the PDFs $f_{Z_0}(y_0|p)$ and $f_{Z_m}(y_m|p)$, the symbol error ratio (SER), which is conditioned on the assumption that p out

of the L hops are jammed by PBNJ, is given by [9]

$$P_s(p) = 1 - \int_0^{\infty} f_{Z_0}(y_0|p) \left[\int_0^{y_0} f_{Z_m}(y_m|p) dy_m \right]^{M-1} dy_0. \tag{32}$$

The overall average SER is therefore given by [3]

$$P_s = \sum_{p=0}^{L} \binom{L}{p} \rho^p (1-\rho)^{L-p} P_s(p). \tag{33}$$

Given the SER, the corresponding BER can be determined using the relation of $P_b = [(M/2)/(M-1)]P_s$ [9].

Alternatively, we can express the conditional SEP as [9]

$$P_s(p) = 1 - \int_0^{\infty} f_{Z_0}(y_0|p) \left[F_{Z_m}(y_0|p) \right]^{M-1} dy_0 \tag{34}$$

where $F_{Z_m}(y_0|p)$ is the CDF of Z_m, $m > 0$, conditioned on p out of the L hops being jammed, and is given by $F_{Z_m}(y_0|p) = \int_0^{y_0} f_{Z_m}(y_m|p) dy_m$. From [12] and [15], we know that the Mellin transform of the integral of a function can be evaluated using the relation

$$\mathcal{M}\left[\int_0^{u} f(x)dx, z \right] = -\frac{1}{z} \mathcal{M}\left[f(x), z+1 \right]. \tag{35}$$

Consequently, from (18) and (35), we have

$$\mathcal{M}\left[F_{Z_m}(y_0|p), z \right] = -\frac{1}{z} \beta_J^{-pz/2} \beta^{-z(L-p)/2} \Gamma^L(z/2+1). \tag{36}$$

Upon taking the inverse Mellin transform of (36) according to (6) and replacing $(z/2+1)$ by z, an expression similar to (24) and (29) can also be derived for F_{Z_m}, which is given by

$$F_{Z_m}(y_0|p) = -\frac{\beta_J^p \beta^{L-p} y_0}{(L-1)!} \sum_{j=0}^{\infty} \sum_{r=0}^{L-1} \binom{L-1}{r} \times \left[\mathcal{U}_{m0}^{(r)}(z) \mathcal{V}_m^{(L-1-r)}(z) \right]_{(z=-j)} \tag{37}$$

where

$$\mathcal{U}_{m0}(z) = \left(\beta_J^p \beta^{L-p} y_0^2 \right)^{-z} \tag{38}$$

and

$$\mathcal{U}_{m0}(z)|_{(z=-j)} = \left(\beta_J^p \beta^{L-p} y_0^2 \right)^{j} \tag{39}$$

whereas its rth derivative $\mathcal{U}_{m0}^{(r)}(z)$ at $z = -j$ is given by

$$\mathcal{U}_{m0}^{(r)}(z)|_{(z=-j)} = \left[-\ln\left(\beta_J^p \beta^{L-p} y_0^2 \right) \right]^r \left(\beta_J^p \beta^{L-p} y_0^2 \right)^j. \tag{40}$$

Furthermore, in (37), we have $\mathcal{V}_m(z) = \mathcal{V}(z)/(z-1)$, whereas its rth-order differential may be expressed, using Leibnitz' rule and a number of further simplifications[16], as

$$\mathcal{V}_m^{(r)}(z)|_{(z=-j)} = -\sum_{t=0}^{r} \binom{r}{t} \mathcal{V}^{(t)}(z)|_{(z=-j)} \frac{(r-t)!}{(1+j)^{r-t+1}} \tag{41}$$

where $\mathcal{V}^{(t)}(z)|_{(z=-j)}$ is given by (28). Given $F_{Z_m}(y_0|p)$, $P_s(p)$ can also be computed using (34), which involves only a single integration, whereas in (32), two integrations have to be computed.

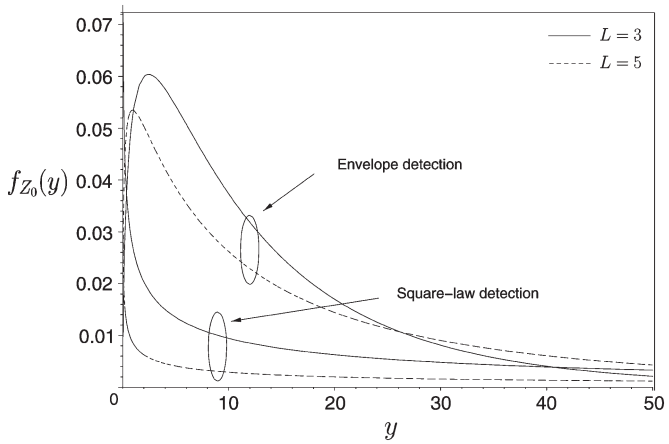

Fig. 2. PDF of the PC's output for both the square-law and envelope detection of the desired tone for an FFH-aided 4-ary FSK PC receiver communicating over an interference-free Rayleigh-fading channel, assuming $L = 3$ and 5 and $E_b/N_0 = 10$ dB.

IV. Analytical Results and Discussion

In this section, we validate our analysis detailed in Section III using analytical and simulation results and discuss the achievable performance of the system employing the proposed method. The integrations seen in (32) and (34) are numerically performed. It has been found, based on our results, that using a limited number of residues, i.e., $j \leq 25$, is sufficient for accurately computing both the PDF and the BER.

Using (24), we portray the PDF of the PC's output corresponding to the FFH-MFSK signal tone in Fig. 2, assuming $M = 4$, $L = 3$ and 5, and $E_b/N_0 = 10$ dB in the absence of jamming. The PDF of the PC's output assuming square-law detection has also been shown using results from [13]. It can be seen in Fig. 2 that beyond a certain value of the PC's output, the envelope detection of the received signal leads to a smaller area under the tail of its PDF compared to the square-law detection. The high probability of encountering high PC output values for square-law detection is due to its squaring operation. By contrast, as observed in Fig. 2, the PDF has a more limited dynamic range when envelope detection is employed. Because accurate numerical integration in (32) and (34) requires the truncation of the PDF at a point where it becomes negligible, the employment of envelope detection facilitates the numerical computation of the BER. We also note from Fig. 2 that the PDFs corresponding to $L = 5$ indicate a lower probability for lower PC outputs than those for $L = 3$, whereas the opposite is true for high PC outputs. This observation holds both for

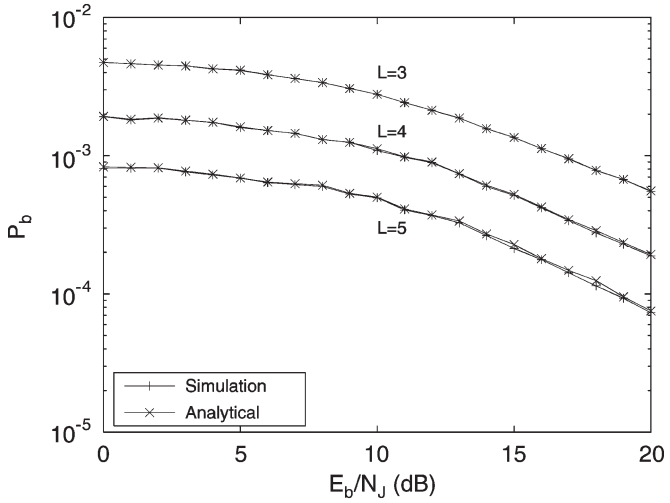

Fig. 3. Comparison of the analytical results obtained using (33) and the simulation results of the BER versus the E_b/N_J performance of an FFH-aided 8-ary FSK PC receiver communicating over a Rayleigh-fading channel, assuming $E_b/N_0 = 20$ dB, $\rho = 0.1$, and various L values.

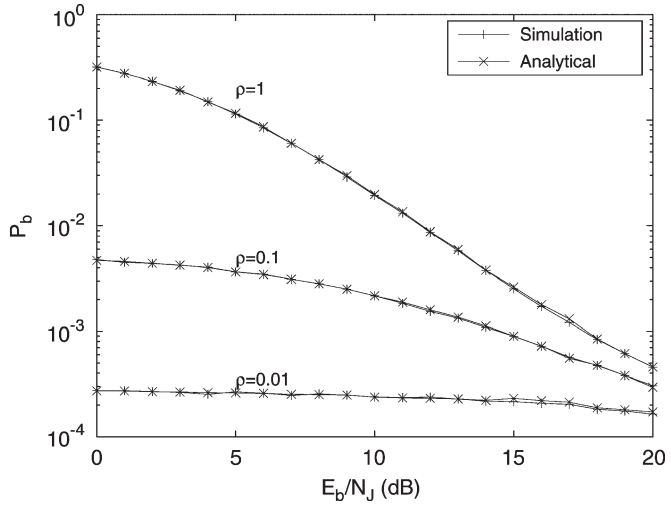

Fig. 4. Comparison of the analytical results obtained using (33) and the simulation results of the BER versus the E_b/N_J performance of an FFH-aided 32-ary FSK PC receiver communicating over a Rayleigh-fading channel, assuming $L = 3$, $E_b/N_0 = 20$ dB, and various values of the PBNJ duty factor ρ.

the envelope and square-law detection and indicates having an increased probability of high PC outputs when a high diversity order is employed.

Using (33) and (34), the effects of increasing the diversity order on the system BER has been characterized in Fig. 3. In this figure, the parameters of $M = 8$, $\rho = 0.1$, and $E_b/N_0 = 20$ dB have been assumed. This figure demonstrates that increasing the value of L enhances the achievable diversity gain, which results in an improved BER. Fig. 3 also demonstrates that our analytical results match the simulation results, although we note in Fig. 3 that at $L = 5$, the analytical results slightly deviate from the simulation results, particularly when E_b/N_J approaches 20 dB. The reason for this inaccuracy is that having a high diversity order prevents the accurate computation of (24), (29), and (34), as explained above. Another reason for the inaccuracy of these results is that the computation of the SER at high values of L incurs higher order differentials, which involve recursive additions (and subtractions) of very large numbers, thus resulting in roundoff errors in the computation of (24) and (37).

In Fig. 4, we have plotted the BER for $M = 32$, $L = 3$, $E_b/N_0 = 20$ dB, and for various values of the PBNJ duty factor ρ. We note from this figure that the BER performance of the system using MFSK follows similar trends to those reported in the context of BFSK in [8]. Specifically, as seen in Fig. 4, $\rho = 1$ results in the worst BER performance, and hence, for $\rho < 1$, a better BER performance is recorded. This observation demonstrates that PBNJ associated with a duty factor of unity constitutes the worst-case jamming scenario in Rayleigh fading. This result is in agreement with previous results on FFH-BFSK PC systems designed for combatting PBNJ [3], [7], [8]. However, note that under less-severe fading conditions or in AWGN, the value of the worst case duty factor may be less than unity, as reported in numerous contributions, including [19]–[24]. Note also in Fig. 4 that as the signal power increases in comparison to the jammer power, the performance of the system becomes less sensitive to ρ.

We also note in Fig. 4 that the analytical results pertaining to $\rho = 0.01$ slightly deviate from the corresponding simulation results. The reason for this difference is that at a low PBNJ duty factor, the effective jammer power encountered in a jammed hop increases, contributing to the increased magnitude of the received signal. Thus, in this scenario, the resultant PC output may become high, and the area under the tail of its PDF may increase. Consequently, under these conditions, the computation of the PDFs and the BER using (24), (29), and (34) may be less accurate.

It has been observed in our investigations that the computation of the BER becomes challenging for $L > 5$, for low values of the jamming duty factor, as well as for E_b/N_J and $E_b/N_0 > 20$ dB, in conjunction with high M, and hence, some numerical precision may have to be sacrificed. Nonetheless, the results are fairly reliable for a wide range of system parameter values of practical interest.

Having validated our analysis using Figs. 3 and 4, we further illustrate the effects of the PBNJ duty factor on the achievable system performance by plotting the BER against ρ in Fig. 5 for $M = 8$ and 64, as well as for $E_b/N_J = 10,\ 15,$ and 20 dB. This figure confirms that $\rho = 1$ constitutes the worst case PBNJ. Furthermore, we note in Fig. 5 that for the relatively high value of $E_b/N_J = 20$ dB, the effect of the jammer duty factor is not as significant as it is when $E_b/N_J = 10$ dB is used. Thus, the BER curves corresponding to $E_b/N_J = 20$ dB are significantly flatter than those for $E_b/N_J = 10$ dB. Another important observation inferred from Fig. 5 is that the lower the duty factor value, the less dramatic the effect of the jammer power on the BER will be. More specifically, observe in Fig. 5 that at low values of the PBNJ duty factor, e.g., at $\rho \approx 0.01$, the BER values recorded are limited to a narrower range regardless of the signal-to-jamming ratio (SJR) value considered. The reason for this trend is that at lower ρ values, PBNJ is not as effective as it is at high values of ρ.

Let us now portray our BER results for various values of the modulation order in Fig. 6, where the parameter values of $L = 3$, $\rho = 0.1$, and $E_b/N_0 = 20$ dB have been assumed. The results of this figure demonstrate that the performance of the

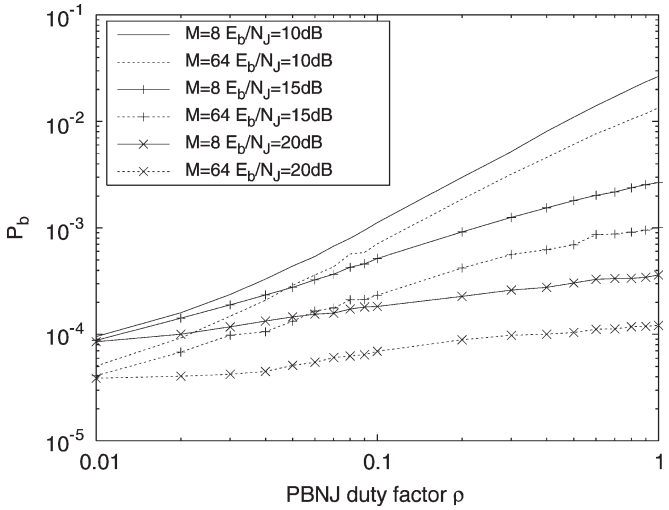

Fig. 5. BER versus the PBNJ duty factor performance of an FFH-aided MFSK PC receiver communicating over a Rayleigh-fading channel, assuming $L = 4$, $E_b/N_0 = 20$ dB, and various values of M and E_b/N_J.

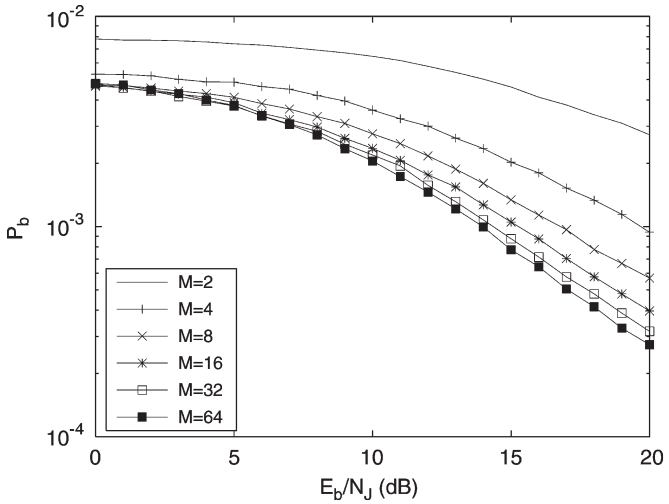

Fig. 6. BER versus the E_b/N_J performance of an FFH-aided MFSK PC receiver communicating over a Rayleigh-fading channel, assuming $L = 3$, $E_b/N_0 = 20$ dB, $\rho = 0.1$, and various M values.

system improves as the modulation order is increased. This result is in agreement with our prior knowledge in the context of M-ary systems [9]. However, only a modest performance improvement is observed in Fig. 6 upon increasing M beyond $M = 16$. Thus, for the sake of striking a good balance between the achievable performance improvement and the bandwidth expansion imposed, $M = 8$ or 16 constitutes a beneficial tradeoff in the context of the system considered.

Let us now quantify the system performance against the worst-case PBNJ, which correponds to $\rho = 1$, as mentioned above in the context of Figs. 4 and 5. In Fig. 7, we plot the BER against E_b/N_J for $\rho = 1$ and for both $M = 2$ and $M = 16$, as well as for various SNR values. Our first observation in Fig. 7 is that the attainable diversity gain is low when the worst-case jamming is encountered, particularly when E_b/N_0 is also low. This observation becomes more explicit upon comparing Figs. 3 and 7, where $\rho < 1$ is assumed and consequently increasing the value of L, results in a significant

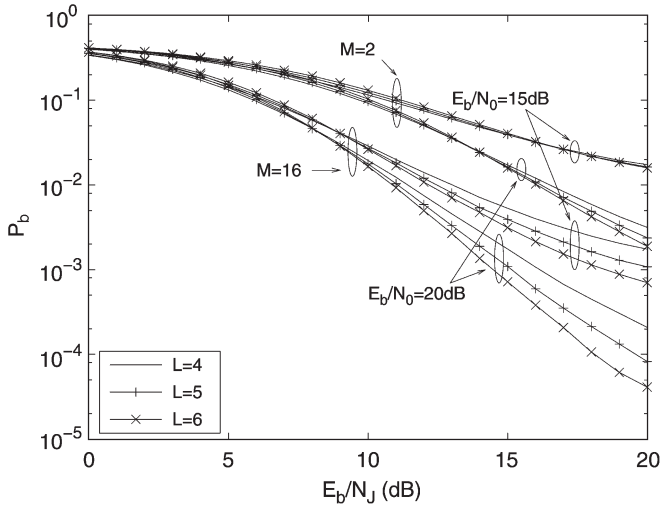

Fig. 7. BER versus the E_b/N_J performance of an FFH-aided MFSK PC receiver communicating over a Rayleigh-fading channel, assuming $\rho = 1$, $M = 2$ and 16, $E_b/N_0 = 15$ and 20 dB, and various L values.

BER improvement. By contrast, we observe in Fig. 7 that initially, no diversity gain is attained, but it becomes more apparent beyond $E_b/N_J \approx 10$ dB. For instance, for $M = 2$ and $E_b/N_0 = 20$ dB, the system using $L = 6$ outperforms $L = 4$ and $L = 5$ when E_b/N_J exceeds 15 dB. This trend has been reported in the context of all FFH-MFSK diversity combining receivers [3], [20]–[24], and it may be physically attributed to the noncoherent combining losses, which limit the diversity gain at a low signal power. We also observe in Fig. 7 that the achievable diversity gain is significant in the case of $M = 16$, whereas corresponding to BFSK, there is hardly any benefit in using higher values of L, particularly at $E_b/N_0 = 15$ dB. This observation demonstrates that, as expected, having an increased modulation order M typically yields a higher diversity gain. Another observation that we may infer from Fig. 7 is that the SNR has a significant effect on the attainable BER performance of the system.

To further characterize the effect of the SNR on the achievable system performance, we plot the system's BER against E_b/N_0 for $L = 5$, as well as for various M and SJR values in Fig. 8. Comparing Fig. 8 with Figs. 3 and 7, our earlier observation that the SNR has a substantial impact on the system's BER is confirmed. More specifically, we note that although in Fig. 3 the BER corresponding to a particular value of L is limited to a narrower range of SJR values spanning from 0 to 20 dB, in Fig. 8, the BER varies with the SNR over a significantly wider range. The reason for the more substantial impact of the SNR on the system's BER is that the detrimental effect of jammer power is limited by another factor, namely by the PBNJ duty factor, as discussed in the context of Fig. 5 above. By contrast, the AWGN is imposed on the transmitted signal under all conditions and thus imposes a more substantial effect on the BER.

V. Conclusion

We have used the Mellin transform to analyze the BER performance of the classic FFH-MFSK PC receiver, operating in a Rayleigh-fading channel contaminated by PBNJ. We have demonstrated that the Mellin transform is a convenient tool to

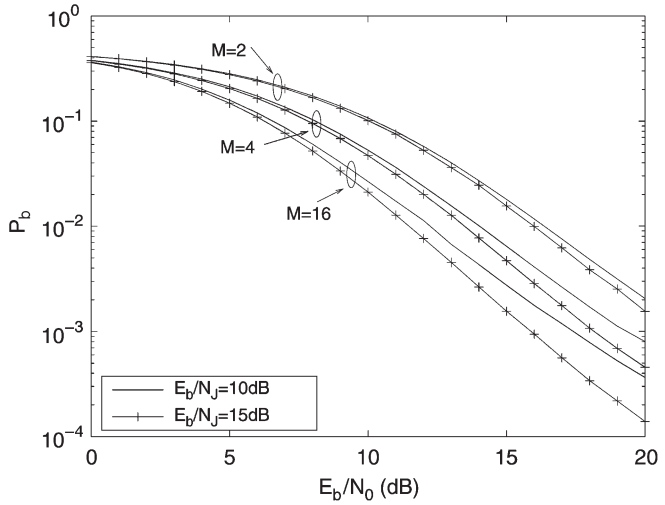

Fig. 8. BER versus the E_b/N_0 performance of an FFH-aided MFSK PC receiver communicating over a Rayleigh-fading channel, assuming $L = 5$, $\rho = 0.1$, $E_b/N_J = 10$ and 15 dB, and various M values.

derive the PDF of a product of random variables. By employing the Mellin-transform-based technique, the PDF and the CDF of the PC's output was determined in a semiclosed form, as seen in (24), (29), and (37). With the aid of these PDF and CDF expressions, the BER of the system has been numerically evaluated, enabling for the first time the analysis of this receiver for $M > 2$. Furthermore, the Mellin-transform-based method provides a convenient expression for computing the PDF of the PC's output, thus providing additional insights, whereas the previous methods proposed in the published literature [3], [7], [8] fall short of providing a solution to this problem. The proposed technique has been shown to be accurate, and the analytical results obtained using (24), (34), and (37) match the simulation results for most practical values of the modulation order, PBNJ duty factor, $L \leq 5$, and E_b/N_J and $E_b/N_0 \leq 20$ dB.

Our analytical results have demonstrated that PBNJ having a jamming duty factor of unity results in the worst-case jamming scenario for the FFH-MFSK system communicating over Rayleigh-fading channels. Moreover, the BER performance of the system improves as either the modulation order or the diversity order is increased. An important observation made through our results is that significantly greater diversity gain can be achieved from FFH if a higher modulation order is employed. Our future research may focus on the investigation of the same system when communicating over more general classes of fading channels, such as Rician or Nakagami-m channels, because the relevant Mellin transforms exist [15].

REFERENCES

[1] K. C. Teh, A. C. Kot, and K. H. Li, "Performance analysis of an FFH/BFSK product-combining receiver under multitone jamming," *IEEE Trans. Veh. Technol.*, vol. 48, no. 6, pp. 1946–1953, Nov. 1999.

[2] K. C. Teh, A. C. Kot, and K. H. Li, "Performance analysis of an FFH/BFSK product-combining receiver with multitone jamming over Rician fading channels," in *Proc. IEEE Veh. Technol. Conf.—Spring*, Tokyo, Japan, May 2000, vol. 2, pp. 1508–1512.

[3] K. C. Teh, A. C. Kot, and K. H. Li, "Partial-band jamming rejection of FFH/BFSK with product combining receiver over a Rayleigh-fading channel," *IEEE Commun. Lett.*, vol. 1, no. 3, pp. 64–66, May 1997.

[4] Y. Han and K. C. Teh, "Error probabilities and performance comparisons of various FFH/MFSK receivers with multitone jamming," *IEEE Trans. Commun.*, vol. 53, no. 5, pp. 769–772, May 2005.

[5] C.-L. Chang and T.-M. Tu, "Performance analysis of FFH/BFSK product-combining receiver with partial-band jamming over independent Rician fading channels," *IEEE Trans. Wireless Commun.*, vol. 4, no. 6, pp. 2629–2635, Nov. 2005.

[6] Y. S. Shen and S. L. Su, "Performance analysis of an FFH/BFSK receiver with product-combining in a fading channel under multitone interference," *IEEE Trans. Wireless Commun.*, vol. 3, no. 6, pp. 1867–1872, Nov. 2004.

[7] T. C. Lim, W. He, and K. Li, "Rejection of partial-band noise jamming with FFH/BFSK product combining receiver over Nakagami-fading channel," *IEEE Commun. Lett.*, vol. 34, no. 10, pp. 960–961, May 1998.

[8] G. Huo and M. S. Aluoini, "Another look at the BER performance of FFH/BFSK with product combining over partial-band jammed Rayleigh-fading channels," *IEEE Trans. Veh. Technol.*, vol. 50, no. 5, pp. 1203–1215, Sep. 2001.

[9] J. G. Proakis, *Digital Communications*. Singapore: McGraw-Hill, 2001.

[10] M. D. Springer, *The Algebra of Random Variables*. New York: Wiley, 1979.

[11] A. M. Mathai, "Products and ratios of generalized gamma variates," *Skand. Aktuarietidskr.*, vol. 55, pp. 193–198, 1972.

[12] I. H. Sneddon, *The Use of Integral Transforms*. New York: McGraw-Hill, 1972.

[13] S. Ahmed, L. L. Yang, and L. Hanzo, "Mellin transform based performance analysis of fast frequency hopping using product combining," in *Proc. IEEE VTC—Spring*, May 2006, vol. 4, pp. 1635–1639.

[14] J. Salo, H. M. El-Sallabi, and P. Vainikainen, "The distribution of the product of independent Rayleigh random variables," *IEEE Trans. Antennas Propag.*, vol. 54, no. 2, pp. 639–643, Feb. 2006.

[15] H. Bateman, *Tables of Integral Transforms*, vol. I. New York: McGraw-Hill, 1954.

[16] I. Gradshteyn and I. M. Ryzhik, *Tables of Integrals, Series and Products*. London, U.K.: Academic, 1965.

[17] P. Galambos and I. Simonelli, *Products of Random Variables: Applications to Problems of Physics and to Arithmetical Functions*. New York: Marcel Dekker, 2004.

[18] S. Lang, *Complex Analysis*. New York: Springer-Verlag, 1999.

[19] P. J. Crepeau, "Performance of FH/BFSK with generalized fading in worst-case partial-band Gaussian interference," *IEEE Trans. Sel. Areas Commun.*, vol. 8, no. 5, pp. 884–886, Jun. 1990.

[20] J. S. Lee, R. H. French, and L. E. Miller, "Probability of error analyses of a BFSK frequency-hopping system with diversity under partial-band jamming intereference—Part I: Performance of square-law linear combining soft decision receiver," *IEEE Trans. Commun.*, vol. COM-32, no. 6, pp. 645–653, Jun. 1984.

[21] J. S. Lee, L. E. Miller, and Y. K. Kim, "Probability of error analyses of a BFSK frequency-hopping system with diversity under partial-band jamming intereference—Part II: Performance of square-law nonlinear combining soft decision receivers," *IEEE Trans. Commun.*, vol. COM-32, no. 12, pp. 1243–1250, Dec. 1984.

[22] L. E. Miller, J. S. Lee, and A. P. Kadrichu, "Probability of error analyses of a BFSK frequency-hopping system with diversity under partial-band jamming intereference—Part III: Performance of a square-law self-normalizing soft decision receiver," *IEEE Trans. Commun.*, vol. COM-34, no. 7, pp. 669–675, Jul. 1986.

[23] R. C. Robertson and T. T. Ha, "Error probabilities of fast frequency-hopped FSK with self-normalization combining in a fading channel with partial-band interference," *IEEE J. Sel. Areas Commun.*, vol. 10, no. 4, pp. 714–723, May 1992.

[24] R. C. Robertson and K. Y. Lee, "Performance of fast frequency-hopped MFSK receivers with linear and self-normalization combining in a Rician fading channel with partial-band interference," *IEEE J. Sel. Areas Commun.*, vol. 10, no. 4, pp. 731–741, May 1992.

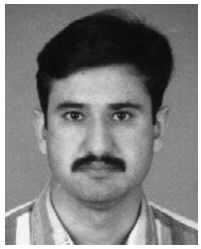

Sohail Ahmed received the M.S. degree in electrical engineering (telecommunications) from the National University of Sciences and Technology, Risalpur, Pakistan, in June 2003 and the Ph.D. degree from the University of Southampton, Southampton, U.K., in August 2007.

He is currently an Associate Professor with the College of Aeronautical Engineering, Risalpur. His research interests include spread-spectrum systems, fast frequency hopping, diversity reception, multiuser detection, and iterative decoding.

Lie-Liang Yang (M'98–SM'02) received the B.Eng. degree in communication engineering from Shanghai Tiedao University, Shanghai, China, in 1988 and the M.Eng. and Ph.D. degrees in electronics and communication engineering from Northern Jiao Tong University, Beijing, China, in 1991 and 1997, respectively.

From June to December 1997, he was a Visiting Scientist with the Institute of Radio Engineering and Electronics, Academy of Sciences of the Czech Republic, Prague, Czech Republic. Since December 1997, he has been with the Communications Research Group, School of Electronics and Computer Science, University of Southampton, Southampton, U.K., where he was a Postdoctoral Research Fellow from December 1997 to August 2002 and a Lecturer from September 2002 to February 2006 and is currently a Reader. He is currently an Associate Editor for the *Journal of Communications and Networks* and the *Journal of Communications*. His research has covered a wide range of areas in telecommunications, which include error-control coding, modulation and demodulation, spread-spectrum communications and multiuser detection, synchronization, space–time processing, and adaptive wireless systems, as well as wideband, broadband, and ultrawideband code-division multiple access. He is the author of over 130 papers in journals and conference proceedings and several book chapters and a coauthor of one book.

Dr. Yang received the Royal Society Sino–British Fellowship in 1997 and the Engineering and Physical Sciences Research Council Research Fellowship in 1998.

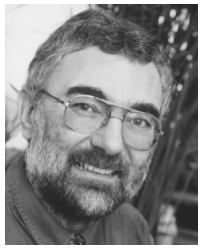

Lajos Hanzo (M'91–SM'92–F'04) received the M.S. degree in electronics and the Ph.D. and D.Sc. degrees in 1976, 1983, and 2004, respectively, all from the University of Southampton, Southampton, U.K.

During his 30-year career in telecommunications, he has held various research and academic posts in Hungary, Germany, and the U.K. Since 1986, he has been with the School of Electronics and Computer Science, University of Southampton, where he is currently the Chair of Telecommunications. He has served as the Technical Program Chair of several IEEE conferences, presented keynote lectures, and has been awarded a number of distinctions.

Dr. Hanzo is currently directing an academic research team working on a range of research projects in the field of wireless multimedia communications sponsored by industry, the Engineering and Physical Sciences Research Council, U.K., the European Information Society Technologies Programme, and the Mobile Virtual Centre of Excellence, U.K. He is an enthusiastic supporter of the liason between industry and academia. He also offers a range of industrial courses. He is a coauthor of 15 John Wiley and IEEE Press books on mobile radio communications, totaling 10 000 pages and is the author of about 750 research papers. He is a Distinguished Lecturer of the IEEE Communications and IEEE Vehicular Technology (VTS) Societies. Since 2005, he has been the Governor of the IEEE VTS, and, since 2008, of ComSoc as well. He serves as an Editor for the PROCEEDINGS OF THE IEEE and as the Editor-in-Chief of the IEEE Press. He is a Fellow of the Royal Academy of Engineering and of the Institution of Electrical Engineers.